THE ROYAL SOCIETY

New high-spin clusters featuring transition metals

By Euan K. Brechin, Alasdair Graham, Paul E. Y. Milne, Mark Murrie, Simon Parsons and Richard E. P. Winpenny

Department of Chemistry, The University of Edinburgh, West Mains Road, Edinburgh EH9 3JJ, UK

Three possible routes to polynuclear transition metal complexes are discussed. The first route, oligomerization induced by desolvation of small cages, is exemplified by synthesis of a dodecanuclear cobalt cage, and by reactions which give octa- and dodecanuclear chromium cages. The second route involves linking cages through organic spacers, and is illustrated by use of phthalate to link together cobalt and nickel cages. For the nickel case a complex consisting of four cubanes and a sodium octahedron is found. The third route involves the use of water to introduce hydroxide bridges into cages. One method of introducing water is to use hydrated metal salts; the transformation of a Cu_6Na cage into a $Cu_{12}La_8$ illustrates this approach. Alternatively, adventitious water within solvents can be used as a source, and this approach has led to a Co_{24} cage. The structures and magnetic properties of these various cages are discussed.

Keywords: high-spin cages; cobalt cages; nickel cages; chromium cages; pyridonates; carboxylates

1. Introduction

The discovery that a polynuclear metal cage can show magnetic hysteresis of a molecular origin is a major step forward in the study of molecular magnetism (Sessoli *et al*. 1993*a*, *b*). Since the original observation of this phenomenon in a Mn_{12} cage it has also been seen in studies of Fe_8 (Barra *et al*. 1996) and tetranuclear manganese (Aubin *et al*. 1996) and vanadium clusters (Sun *et al*. 1998). More detailed analysis has also revealed quantum tunnelling of the magnetization in the Mn_{12} (Friedman *et al*. 1996; Thomas *et al*. 1996) and Fe_8 cages (Sangregorio *et al*. 1997). The slow relaxation of magnetization within a molecular species represents the ultimate in miniaturization of a 'magnetic memory', while the observation of quantum effects within crystalline materials allows detailed analysis of the mechanism of quantum tunnelling. Thus these results have great fundamental importance, and great technological potential.

For a synthetic coordination chemist there are several challenges. The simplest is to provide more and more varied 'single-molecule magnets' for the physicists to study. Variations have included integer and non-integer spin ground states (Aubin *et al*. 1998), and spin ground states varying from $S = 3$ to $S = 10$. It would also be attractive to create cages with new shapes and examine how the topology of the cage influences the magnetic properties. A further task is to increase the spin of the ground

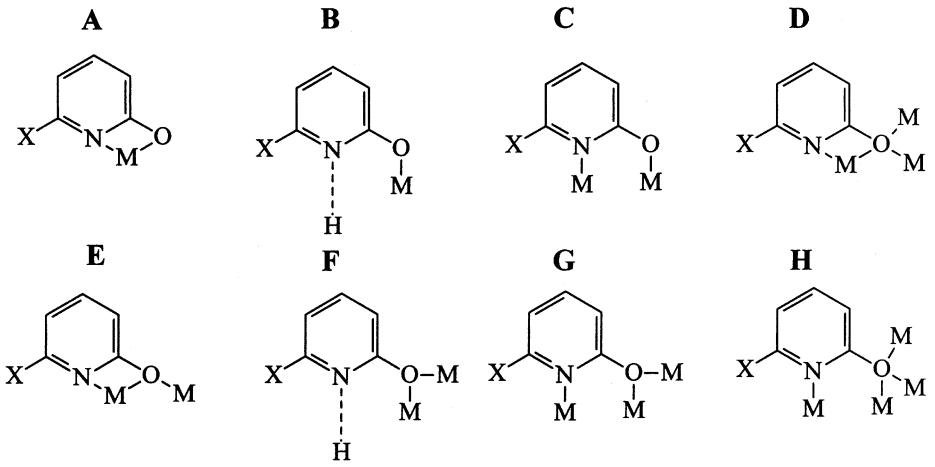

Figure 1. Possible binding modes for pyridonate ligands.
Abbreviations used: X = Cl, chp; X = Me, mhp.

states, which should lead to a higher blocking temperature below which molecules can function as magnets. The most likely route to a higher-spin ground state is via larger paramagnetic cages; therefore, coordination chemists need to learn how to make bigger cages. Underlying every challenge is the fundamental difficulty of the area, which is that designed synthesis is rarely possible. Therefore another aspect of such research is to learn to move beyond serendipity and towards designed synthesis. Here one aspect of the work taking place in Edinburgh is discussed: possible routes to larger cages.

2. Possible routes to larger cages

Compared with the massive cages made with diamagnetic metals, e.g. the polyoxometallate cages synthesized by the Müller group (Müller *et al*. 1998), or the chalcogenide clusters made by the Fenske group (Fenske *et al*. 1998), cages which contain exclusively paramagnetic metal centres are very limited in size. The most paramagnetic centres assembled in one molecule is around 20, and no group at present seems able to make and crystallize a larger compound. Our work has not got far beyond this limit, but results achieved may suggest new pathways to explore.

(*a*) *Oligomerization induced by desolvation*

It is noticeable that for many small cages growth is terminated by coordination of solvate molecules. This suggests that if the solvate molecules could be removed by heating, oligomerization may occur as remaining ligands adjust their coordination modes to satisfy the coordination number demanded by the metal sites. Ligands based on substituted pyridonates are in many ways ideal as coligands for such studies, as the pyridonates show a wide range of bonding modes (figure 1).

The initial studies we carried out were on a tetranuclear cobalt heterocubane which can be readily crystallized from MeOH (Brechin *et al*. 1996*b*). The cage has formula $[Co_4(\mu_3\text{-OMe})_4(chp)_4(MeOH)_7]$ **1** (where chp = 6-chloro-2-pyridonate, i.e. X = Cl

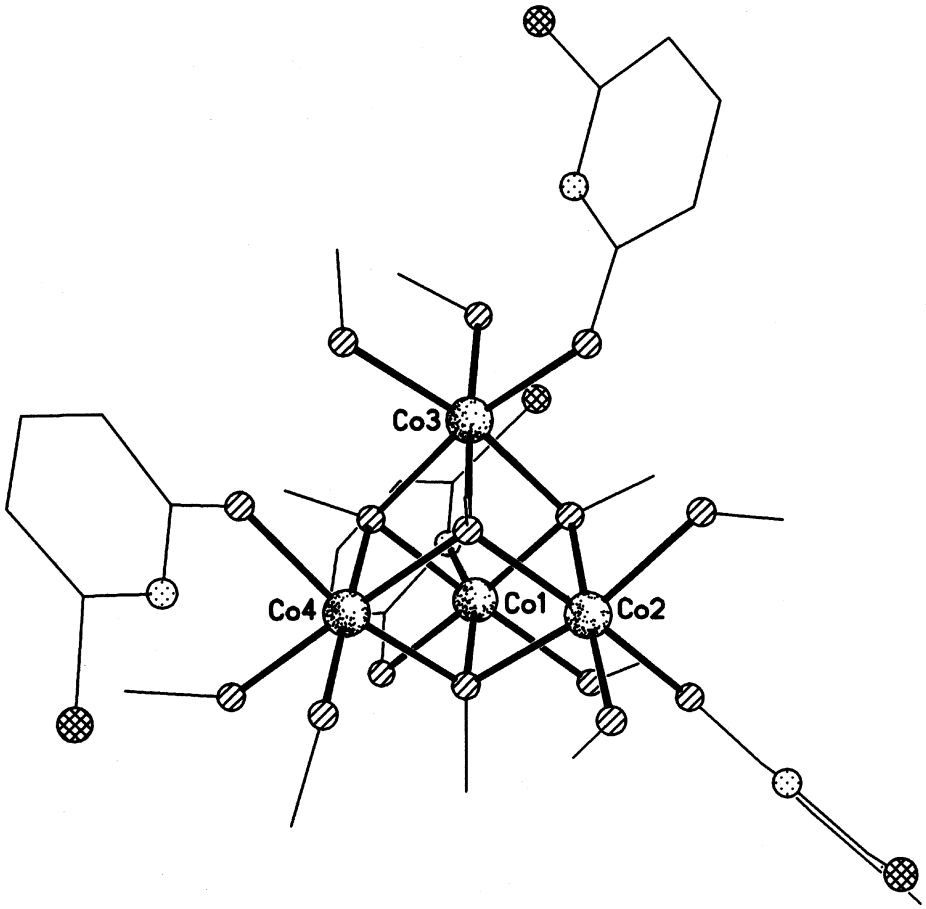

Figure 2. The structure of **1** in the crystal.

in figure 1), and crystallizes with seven terminally bound MeOH ligands. Three of the four chp ligands adopt bonding mode B, while the fourth has mode A (figure 2). Heating the sample prior to crystallization, followed by crystallization from a non-coordinating solvent, drives off most of the coordinated MeOH molecules, leading to a centrosymmetric dodecanuclear cage $[Co_{12}(chp)_{18}(OH)_4(Cl)_2(Hchp)_2(MeOH)_2]$ **2**. This compound has a more complex structure, and in figure 3 both the whole molecule and the metal–oxygen core are shown. As can be seen, the centrosymmetric cage contains two $[Co_4O_3Cl]$ cubes (containing Co(2), Co(3), Co(4) and Co(5)) linked by a central eight-membered ring involving four Co (Co(5) and Co(6) and symmetry equivalents) and four O atoms. The pyridonate ligands in **2** adopt bonding modes **B**, **D**, **E** and **G**. Thus, desolvating the original cage has led to a larger oligomer supported by the coordinative flexibility of the pyridonates.

The second example of this approach involves chromium carboxylates. The oxo-centred triangular cages of formula $[Cr_3O(O_2CR)_6L_3]^+$ can be made with a wide variety of carboxylates. When L is water or a mixture of water and hydroxide, we have found that heating the cages to between 200 and 400 °C in a stream of dry

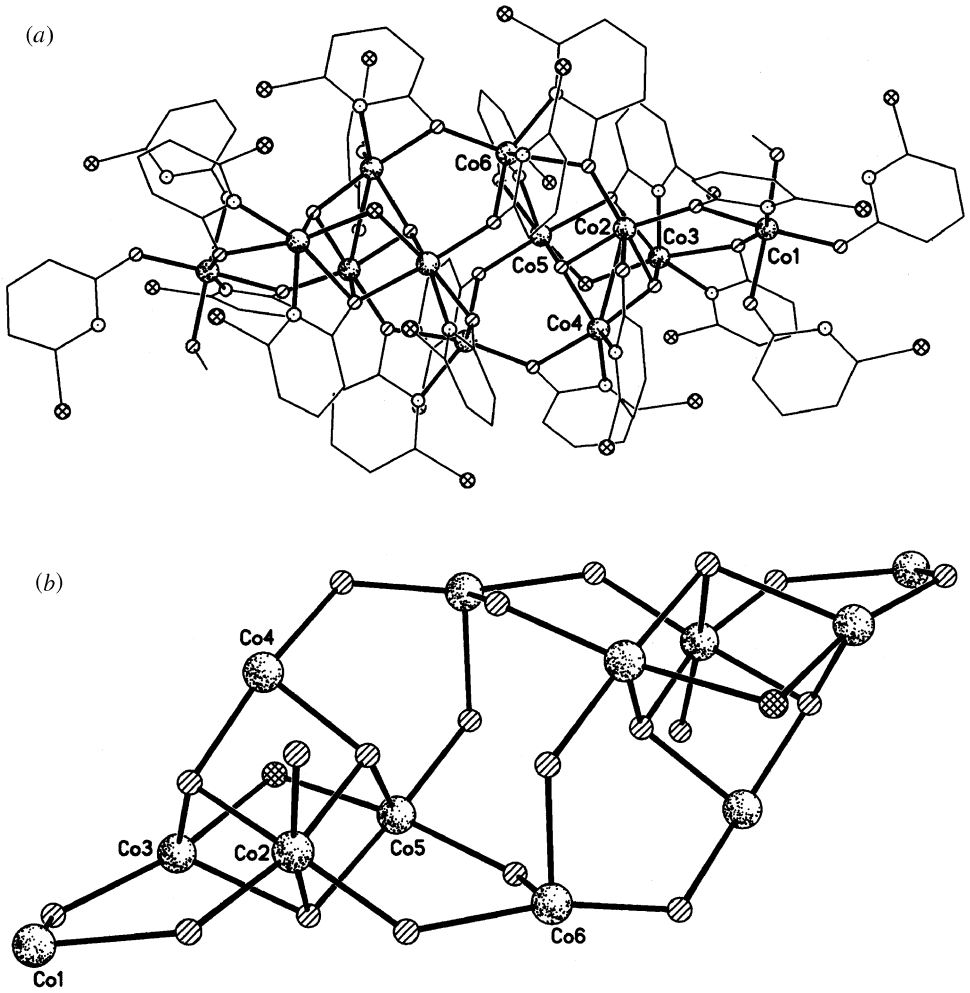

Figure 3. (*a*) The structure of **2** in the crystal; (*b*) metal–oxygen core in **2**, showing the linked cubanes.

nitrogen or under vacuum causes elimination of either water or the carboxylic acid, leading to oligomerization (Atkinson *et al*. 1999).

For example, heating $[Cr_3O(O_2CPh)_6(H_2O)_2(OH)]$ to 210 °C, followed by extraction with CH_2Cl_2 and crystallization gives an octanuclear chromium wheel $[Cr(OH)(O_2CPh)_2]_8$ **3** (figure 4). In **3** each Cr···Cr vector is bridged by one μ_2-hydroxide and two 1,3-bridging benzoates. The equivalent reaction, but heated to 400 °C, generates a more compact cage, $[Cr_8O_4(O_2CPh)_{16}]$ **4**, which contains a Cr_4O_4 heterocubane (containing Cr(1), Cr(2), Cr(3) and Cr(4)), with each oxide bound to an additional Cr centre—creating a second larger Cr tetrahedron outside the core of the cage (figure 5). Four benzoate ligands are chelating, and the remaining twelve bridge Cr···Cr vectors.

Although the yield of **3** is low, **4** is formed almost quantitatively, and it is worth

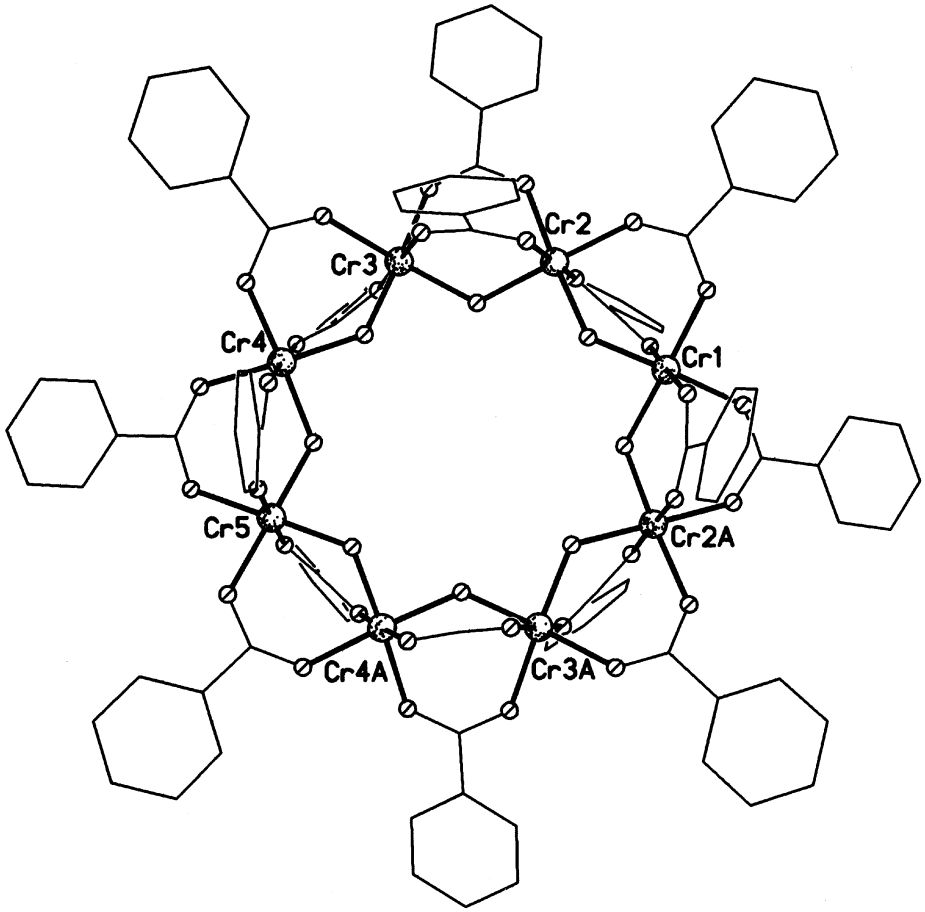

Figure 4. The structure of **3** in the crystal. A crystallographic two-fold axis passes through Cr(1) and Cr(5).

attempting a mass balance for the two reactions:

at 210°C, $8[Cr_3O(O_2CPh)_6(H_2O)_2(OH)] \rightarrow 3[Cr(\mu_2\text{-}OH)(O_2CPh)_2]_8 + 8H_2O$;

at 400°C, $8[Cr_3O(O_2CPh)_6(H_2O)_2(OH)] \rightarrow 3[Cr_8(\mu_4\text{-}O)_4(O_2CPh)_{16}] + 20H_2O$.

Given the low yield of **3** this is a little tendentious, but it does illustrate that the difference between the two reactions is the degree of dehydration of the original chromium triangle.

The same reaction but using pivalate (trimethylacetate) as the carboxylate was reported several years ago by the Gérbéléu group (Batsanov *et al*. 1991), giving a dodecanuclear cage. We have re-examined this synthesis and characterized the cage by both X-ray and neutron diffraction in order to find all protons and hence assign oxidation states for the chromium centres. As a result, we believe the cage should be formulated as $[Cr_{12}O_9(OH)_3(O_2CCMe_3)_{15}]$ **5**. The structure, which has crystallographic D_3 symmetry, consists of a centred-pentacapped-trigonal prism of chromium centres (figure 6). The central chromium (Cr(1)) is bound to six μ_4-oxides,

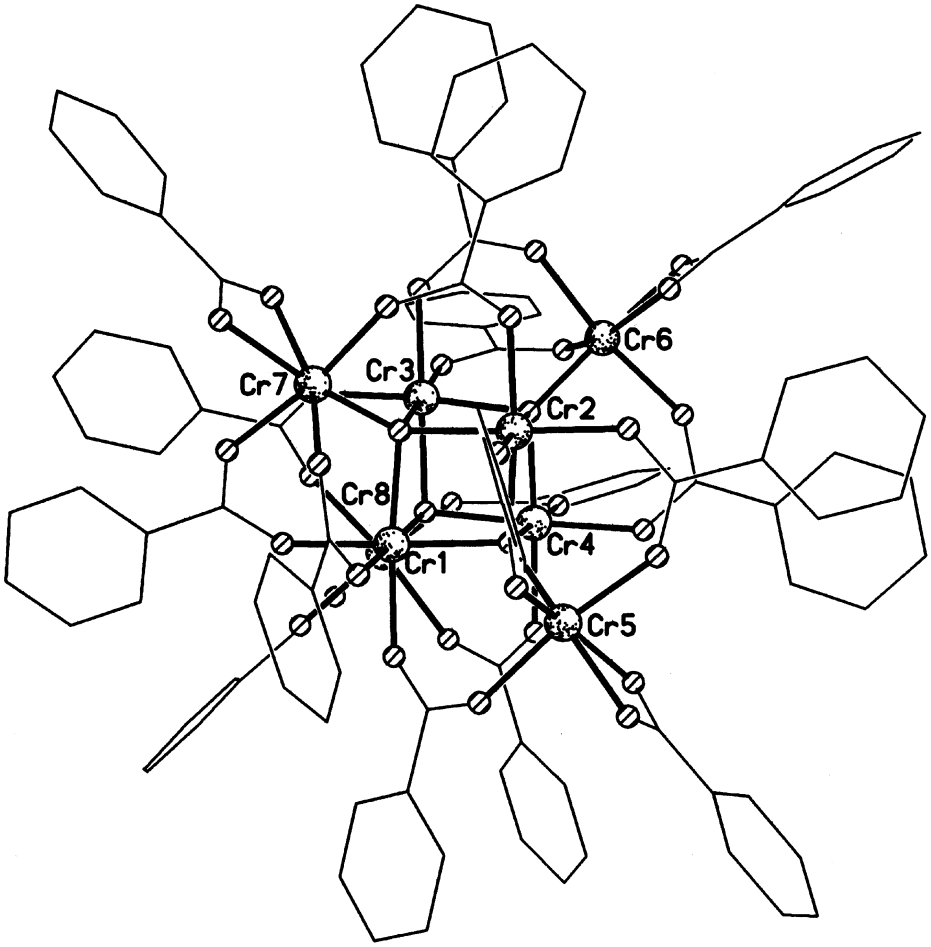

Figure 5. The structure of **4** in the crystal. A crystallographic two-fold axis passes through Cr(1) and Cr(5).

which bridge to one vertex (e.g. Cr(4)), one triangular face-capping (e.g. Cr(2)) and one rectangular face-capping site (e.g. Cr(3)). There are also six μ_3-oxygen sites, which each bridge two vertex and one rectangular face-cap. Neutron studies show that a half-weight proton is attached to each of these six sites, indicating a positional disorder and that each position should be regarded as equal occupancy oxide/hydroxide. The pivalate ligands 'coat' the surface of the cage.

The yield of **5** is extremely high, and carrying out a similar mass balance as for the benzoate cages reveals a surprising difference in the synthesis of **5**:

$$4[Cr_3O(O_2CCMe_3)_6(H_2O)_2(OH)] \rightarrow [Cr_{12}(\mu_4\text{-}O)_3(\mu_3\text{-}OH)_9(O_2CCMe_3)_{15}]\ \mathbf{5} + 9HO_2CCMe_3.$$

Here, rather than loss of water, the carboxylic acid is removed by heating to 400 °C. This suggests that greater variation of the carboxylates present might generate fur-

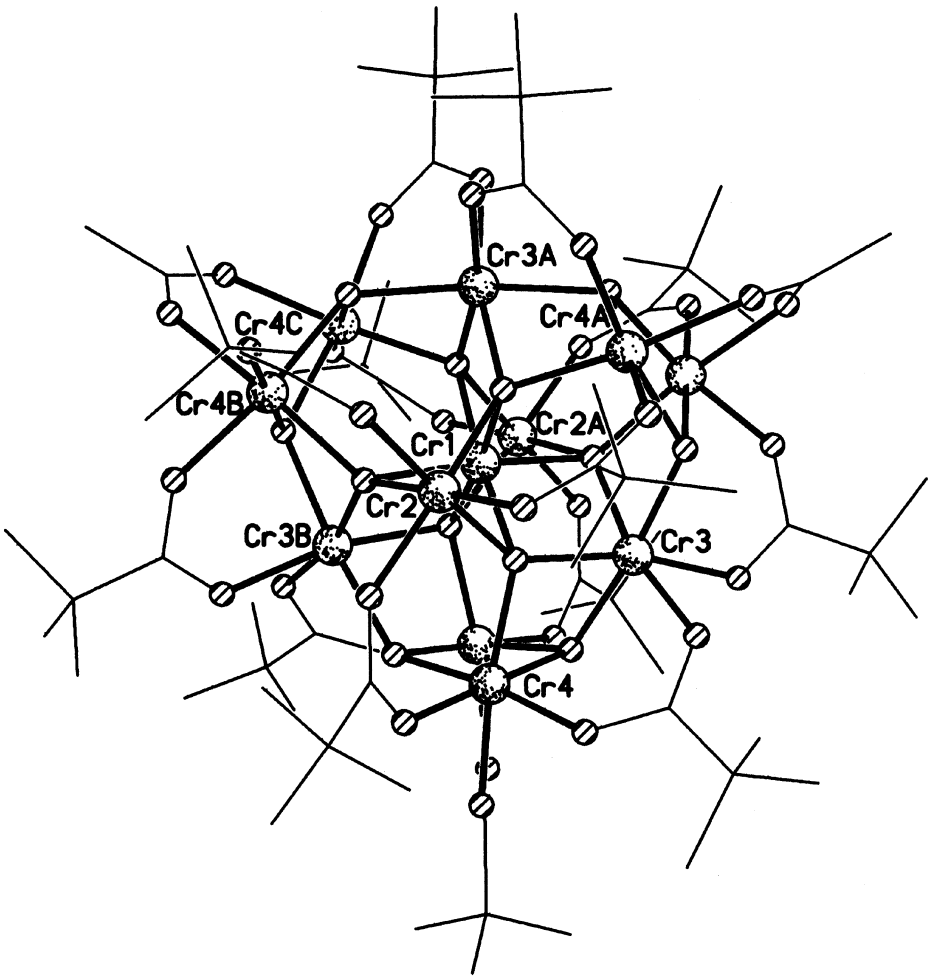

Figure 6. The structure of **5** in the crystal. A crystallographic three-fold axis passes through Cr(1) and Cr(2), and three two-fold axes pass through Cr(1) and Cr(3) and its symmetry equivalents.

ther chromium cages. It is unclear why pivalic acid is removed in the latter case where water was lost in the earlier examples.

The magnetic susceptibilities of **3**, **4** and **5** have been measured from 1.8 to 300 K. For **3** the susceptibility data could be modelled using the Hamiltonian $H = JS_xS_{x+1} + JS_8S_1$ $(1 \leqslant x \leqslant 7)$ with $J = 12.0\,\mathrm{cm}^{-1}$. For **4** a more complex Hamiltonian is required:

$$H = J_1(S_1S_2 + S_1S_3 + S_1S_4 + S_2S_3 + S_2S_4 + S_3S_4) + J_2\{S_5(S_1 + S_2 + S_4) + S_6(S_2 + S_3 + S_4) + S_7(S_1 + S_2 + S_3) + S_8(S_1 + S_3 + 4)\},$$

where J_1 is the exchange between Cr atoms in the central heterocubane, and was found to be $2.1\,\mathrm{cm}^{-1}$, and J_2 models the exchange between the central Cr atoms

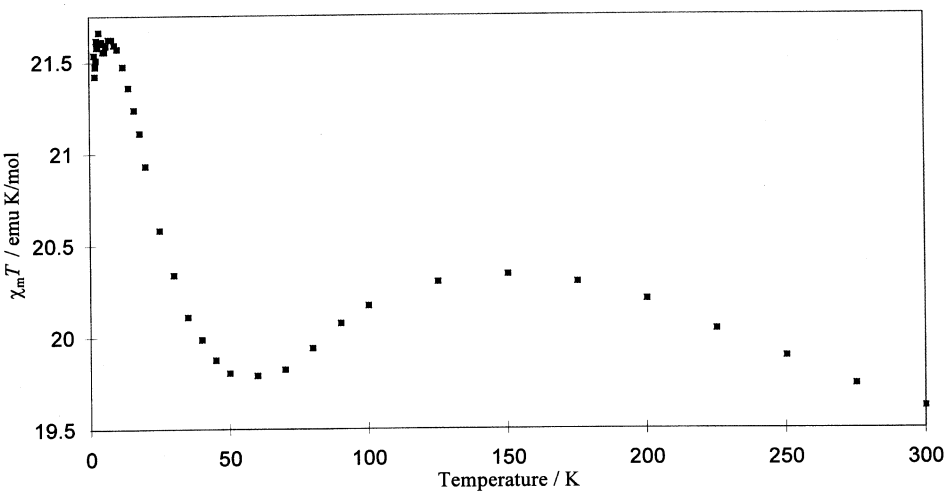

Figure 7. $\chi_m T$ (cm^3 K mol^{-1}) plotted against T (K) for **5**.

and the outer tetrahedron, and was found to be 3.4 cm^{-1}. In both cases essentially diamagnetic ground states result.

For **5** the susceptibility behaviour is more interesting (figure 7). The plot of $\chi_m T$ against T shows a double maxima at *ca.* 150 and *ca.* 10 K. The value of the lower temperature maximum (21.6 cm^3 K mol^{-1}) suggests an $S = 6$ ground state ($\chi_m T$ calculated for $g = 1.99$ and $S = 6$ is 20.8 cm^3 K mol^{-1}). The complexity of the structure makes modelling this behaviour impossible at present. Confirmation of the ground state comes from EPR studies. At low temperature, and for all frequencies studied (24, 34, 90, 180 GHz), a complex multiplet is observed. The 90 GHz spectrum can be simulated with the spin-Hamiltonian parameters: $S = 6$, $g_{zz} = 1.965$, $g_{xx} = g_{yy} = 1.960$, $D = +0.088$ cm^{-1}, $E = 0$ (where D and E are the axial and rhombic zero-field splitting parameters, respectively). Unfortunately, the sign of D indicates that **5** is a high-spin cage but not a single-molecule magnet.

(*b*) *Linking cages into supracages*

Heating small cages to moderate or high temperatures is one means to cause oligomerization. A second method would be to add a linker to join the cages together. Given our success with ligands such as pyridonates and carboxylates, we examined this route using phthalate as the linker. Previous work using phthalate has been published by the Christou group (Squire *et al.* 1995). Here two examples are discussed, one with cobalt and one with nickel.

The cobalt chemistry (Brechin *et al.* 1996*b*) illustrates the new structures which can result when phthalate is included in reactions previously performed with monocarboxylates. Reaction of cobalt chloride with sodium benzoate and Na(chp) in MeOH, followed by recrystallization from MeCN, gives a heptanuclear cobalt cage $[Co_7(OH)_2(O_2CPh)_4(chp)_8(MeCN)]$ **6** (figure 8). Similar cages can be formed with trimethylacetate as the carboxylate. The polyhedron is extremely irregular, and is probably best described as based on a square-based pyramid (Co(1), Co(1A), Co(4), Co(4A), Co(2)), capped on one edge of the square-base (Co(5)) and on the neigh-

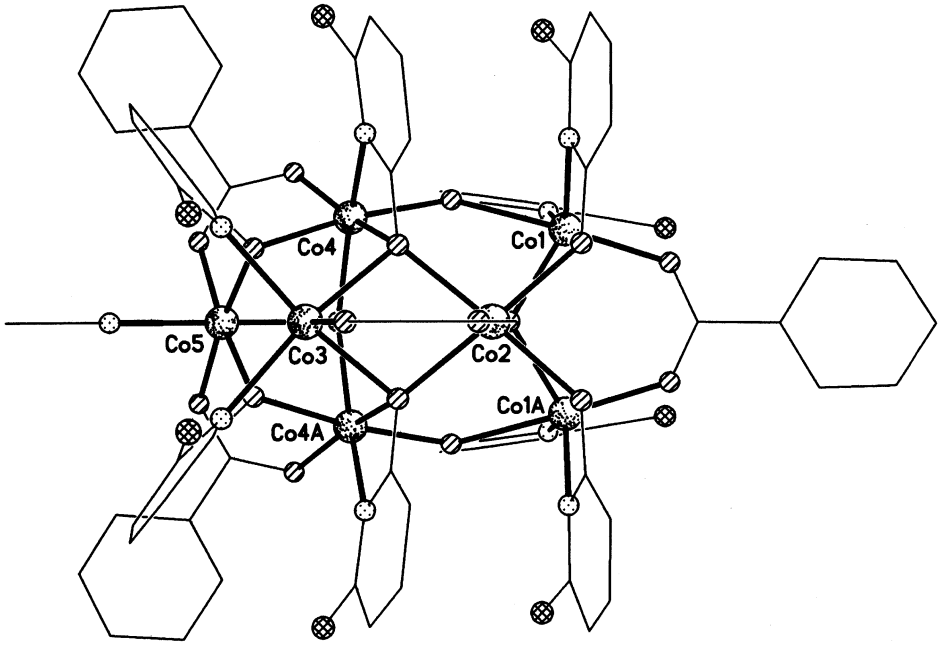

Figure 8. The structure of **6** in the crystal. Co(2), Co(3) and Co(5) lie on a mirror plane.

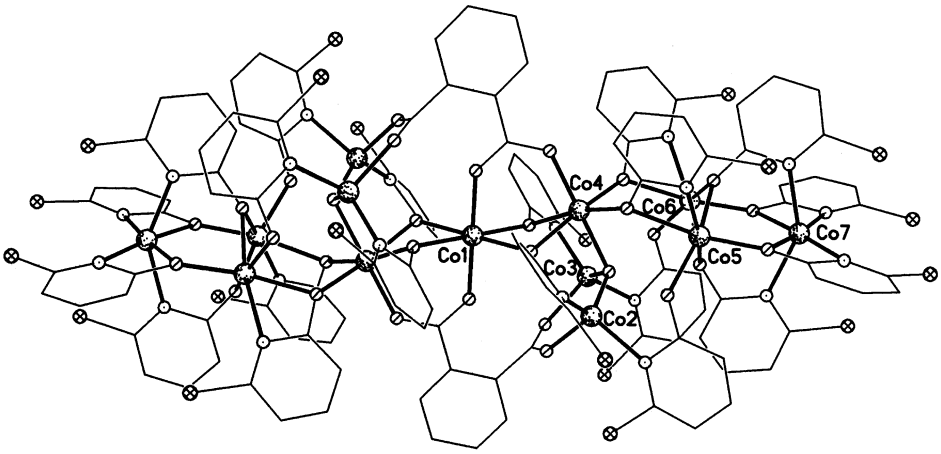

Figure 9. The structure of **7** in the crystal. Co(1) is on an inversion centre.

bouring triangular face (Co(3)). While the benzoate ligands in **6** all bridge in a 1,3-manner, the chp ligands adopt bonding modes **C**, **D**, **E** and **G**.

Substituting sodium phthalate in place of $Na(O_2CPh)$ in the reaction which gives **6** leads to a larger cage, $[Co_{13}(OH)_2(phth)_2(chp)_{20}]$ **7** (where phth is phthalate) (figure 9). The structure is complex and highly irregular. The cage crystallizes with a central Co atom (Co(1)) sitting on an inversion centre. This cobalt is bound to two phth ligands which link to the two halves of the cage. The remainder of the cage

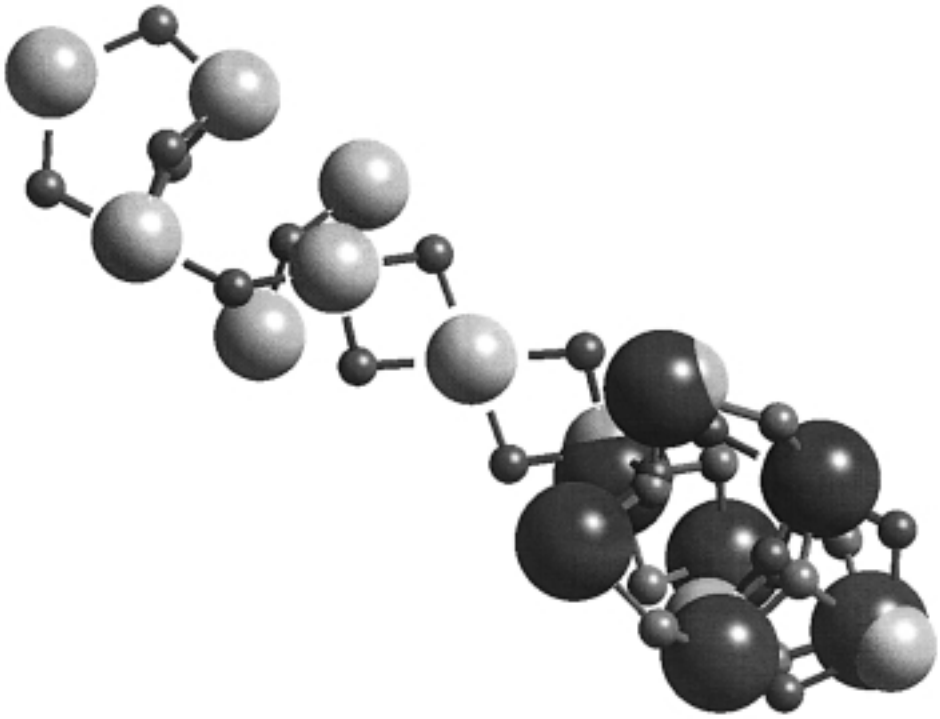

Figure 10. Superposition of the metal–oxo cores of **6** and **7** showing the resemblance between the cages: lighter balls, complex **7**; darker balls, complex **6**.

is 'coated' with chp ligands which adopt three bonding modes: **C**, **E** and **G**. Initial examination of the structure suggests no relationship between **6** and **7**; however, matching the metal–oxo cores of the two reveals a surprising degree of overlap. Figure 10 shows a superposition of the two cores. At the upper left of the figure is one asymmetric unit of **7**. At the lower right of the figure the core of **6** is superimposed on the second-half of **7**. Six of the Co centres in **6** find an excellent fit with the six centres in **7** which are in general positions. The metal capping the triangular face of the square-based pyramid in **6** (Co(3)), and the cobalt atom on the inversion centre (Co(1)) in **7** do not find good matches. It is therefore reasonable to imagine **7** as a 'dimer' of **6**, linked through phthalates. In both structures the immense coordinative flexibility of the pyridonate ligands is crucial in allowing the formation and crystallization of these unusual structures.

While the cobalt chemistry illustrates what might be expected when a linking group is substituted for another component of a reaction, the nickel chemistry illustrates what might happen when such a ligand is simply added to a reaction. The reaction in question is a simple one. Nickel chloride reacted Na(chp) in MeOH gives a heterocubane, $[Ni_4(OMe)_4(chp)_4(MeOH)_7]$ **8**, which is isostructural with **1** (figure 2) (Blake *et al*. 1995). If sodium phthalate is added to the reaction a heterometallic complex crystallizes of formula $[Ni_{16}Na_6(OMe)_{10}(chp)_4\ (OH)_2(phth)_8(Hphth)_2(MeOH)_{20}]$ **9** (figure 11) (Brechin *et al*. 1996*a*). The compound retains the nickel heterocubanes, linked through phthalate bridges, but unexpectedly an Na_6

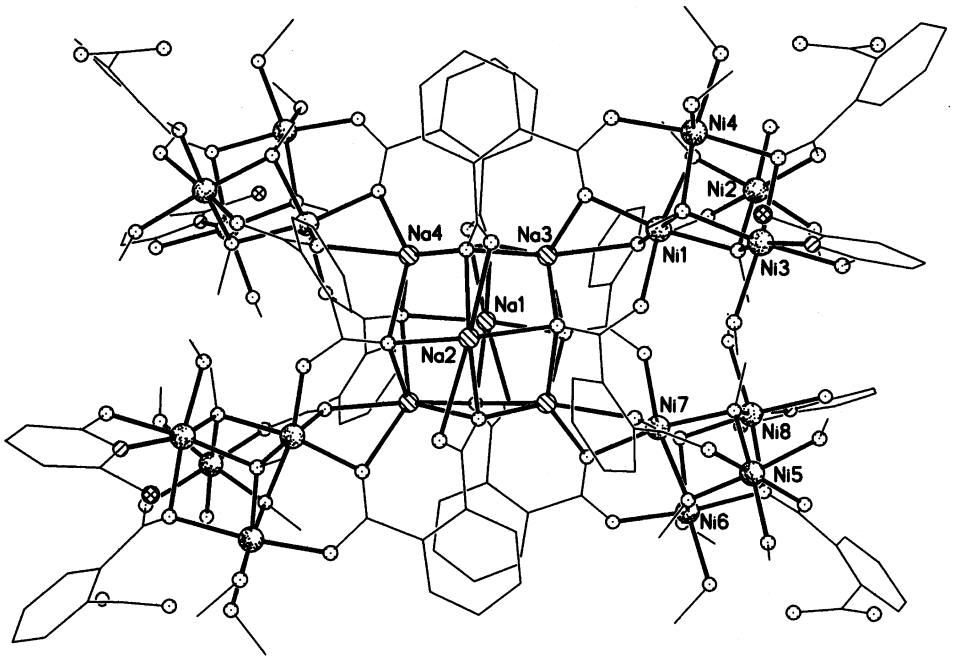

Figure 11. The structure of **9** in the crystal. A crystallographic two-fold axis passes through Na(1) and Na(2).

octahedron forms at the centre of the cage. Therefore the phthalates connect five cages—four cubanes and an octahedron.

The result is intriguing when considered in conjunction with the synthesis of $[Co_{12}(chp)_{18}(OH)_4(Cl)_2(Hchp)_2(MeOH)_2]$ **2**, which is also formed from reaction of a heterocubane (see § 2 *a*). Heating a heterocubane drives off neutral solvent molecules, causing oligomerization through modifying the bonding modes of the pyridonate ligands, while adding a charged linker such as phthalate displaces charged terminal pyridonate ligands, causing oligomerization in a quite different way. In principle the cubanes are building blocks which can be assembled into different higher-nuclearity cages depending on the method used for the assembling.

The magnetic properties of **9** are rather disappointing. Over the temperature range 300–25 K, $\chi_m T$ rises steadily from close to a value expected for 16 non-interacting $S = 1$ centres (19.4 cm^3 K mol^{-1} for $g = 2.2$), to a maximum of 22.1 cm^3 K mol^{-1}. Below 25 K $\chi_m T$ falls rapidly. The simplest explanation for the behaviour is to consider each Ni_4 cubane separately. The spin ground state of each is probably $S = 2$, based on correlation of coupling with bond angle (Halcrow *et al.* 1995). The rise in $\chi_m T$ as the temperature falls to 25 K is due to depopulation of the $S = 0$ and 1 energy levels; the fall after 25 K is probably due to depopulation of the $S = 4$ and $S = 3$ levels. There is no evidence for interaction between the four cubanes in the structure.

(*c*) *Serendipitous solvolysis*

Perhaps the best bridging ligands for synthesis of large cages are oxides and hydroxides. The problem in using them in synthesis is the insolubility of the relevant metal

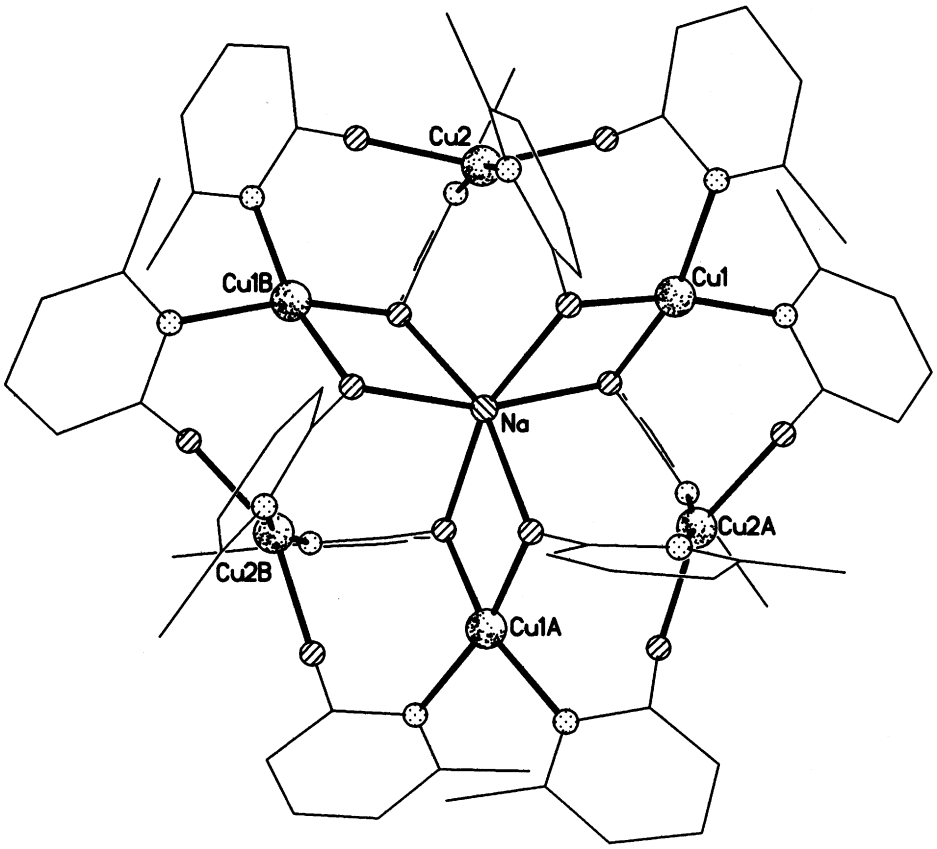

Figure 12. The structure of the cation of **10** in the crystal. A crystallographic three-fold axis passes through Na.

oxides, oxy-hydroxides and hydroxides. We have been exploring a number of reactions where hydrolysis takes place during crystallization. These results suggested it might be worth examining reactions where other solvents attack complexes causing growth of larger cages.

One possible source of water to cause hydrolysis is hydrated metal salts. The only example we have of where this works is the conversion of $[Cu_6Na(mhp)_{12}][NO_3]$ **10** (where mhp is 6-methyl-2-pyridonate, X = Me in figure 1), into $[Cu_{12}La_8(OH)_{24}(NO_3)_{22}(Hmhp)_{13}(H_2O)_6][NO_3]_2$ **11** by reaction with hydrated lanthanum nitrate (Blake *et al*. 1997). **10** contains a hexanuclear copper core surrounding a sodium centre with a 'star of David' array (figure 12). This complex is soluble in CH_2Cl_2, and reacts with solid lanthanum nitrate to give blue crystals of **11** (figure 13). **11** contains a cube of La centres surrounding a Cu_{12} cuboctahedron with each $LaCu_2$ triangle containing a central hydroxide bridge. The core is thus $[Cu_{12}La_8(OH)_{24}]^{24+}$, with all other ligands attached to the remaining coordination sites of the La centres. While the core has non-crystallographic O_h symmetry the exterior ligands are extremely disordered. Although this reaction looks potentially very exciting, it has proved difficult to extend to other systems.

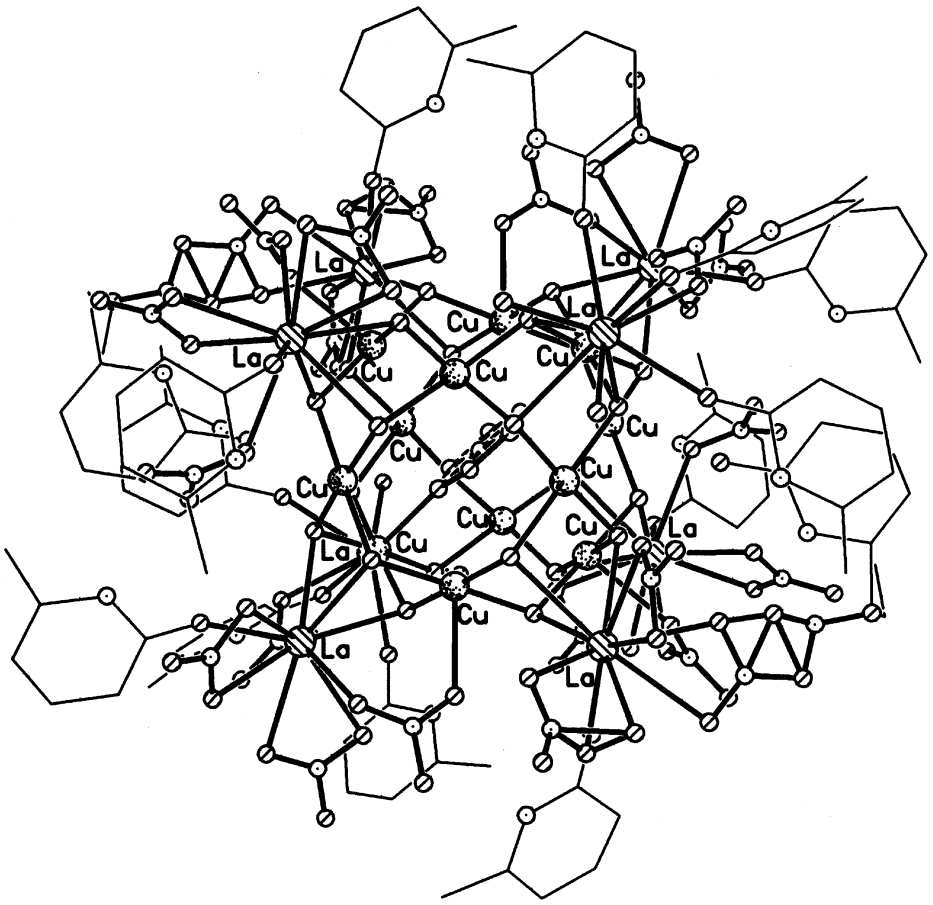

Figure 13. The structure of the cation of **11** in the crystal. The structure is centrosymmetric.

A second, and more productive source of adventitious water, is solvent. Solvents such as ethyl acetate contain *ca.* 1–3% water unless dried carefully. This amount of moisture seems suitable for solvolysis reactions. For example, reaction of anhydrous cobalt chloride with Na(mhp) in MeOH gives a purple solution which can be evaporated to dryness and redissolved in ethyl acetate. From the resulting purple solution, large purple crystals form after a period of days. The resulting cage, $[Co_{24}(OH)_{18}(mhp)_{22}(OMe)_2(Cl)_6]$ **12** (figure 14), resembles a fragment of cobalt hydroxide (Brechin *et al.* 1997). The cage contains sixteen cobalt centres which are based on octahedral coordination geometries (Co(1), Co(2), Co(3), Co(4), Co(5), Co(6), Co(7), Co(8) and symmetry equivalents), with varying amounts of distortion, while the remaining eight cobalt sites have distorted tetrahedral geometries. The central region of the cage contains the octahedral sites, bridged mainly by μ_3-hydroxides and some μ_3-methoxides and chlorides. The circumference of the disc has mhp ligands attached, showing bonding modes **C**, **E** and **G**. Again, the flexibility of the ligand helps support formation of the cage. The magnetic behaviour of **12** seems unusual, with a divergence between field-cooled and zero-field-cooled susceptibility

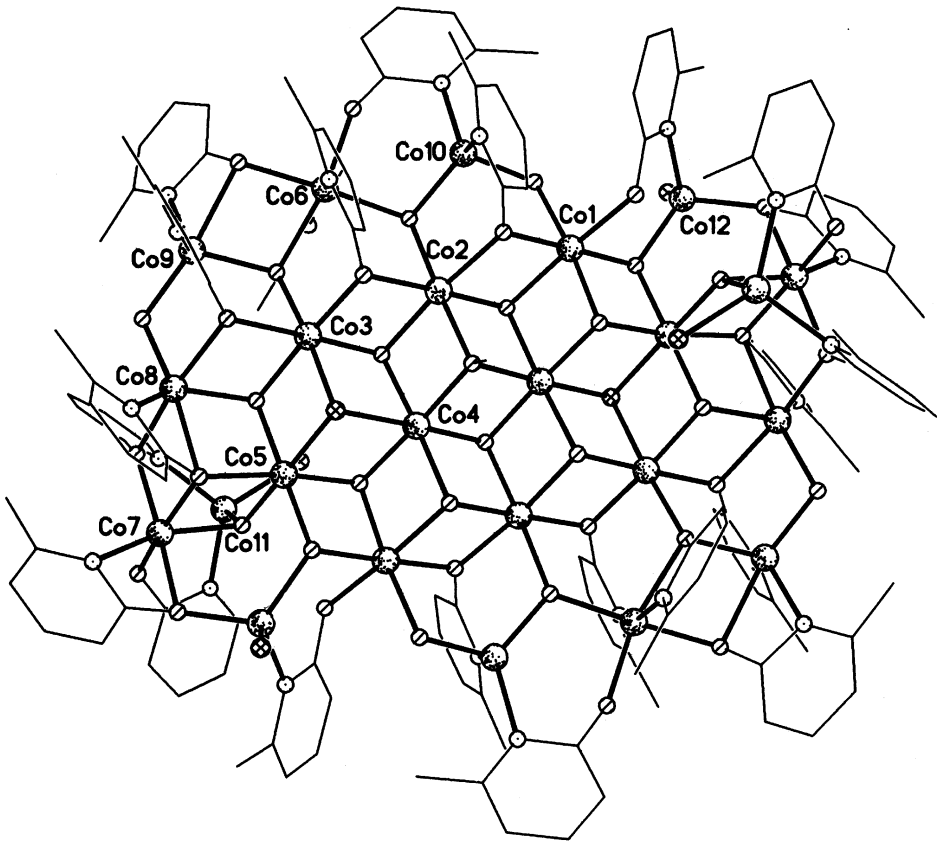

Figure 14. The structure of **12** in the crystal. The structure is centrosymmetric.

at 4.5 K. Whether this is of a molecular origin, or is evidence of spin-glass behaviour is open to question. The molecules of **12** pack efficiently in the crystal, and intermolecular interactions are likely to be important in determining the bulk magnetic properties.

12 contains 24 paramagnetic centres, which makes it one of the largest cages crystallographically characterized to date. We therefore spent some time examining the reaction which gives **12**, and in attempting to make analogous cages for nickel. The amount of moisture present is crucial in forming and crystallizing **12**: too much moisture and an insoluble product forms which appears to be, in the main, cobalt hydroxide. We also attempted to exclude moisture, and although we failed we found another new cage, $[Co_9(OH)_4(mhp)_8(Cl)_6(Hmhp)_4]$ **13** (figure 15). The structure does not resemble **12** closely, although there are common features. **13** crystallizes on a two-fold axis, with a central cobalt atom (Co(1)) lying on the symmetry element. Co(1) is part of two vertex-sharing cubanes which are both distorted as one cobalt (Co(5)) is slightly out of position. Co(5) and Co(4) have tetrahedral coordination geometries, while Co(1) and Co(2) have octahedral geometries and Co(3) is extremely irregular. This mixture of coordination environments is also found in **12**. The mhp ligands in **13** adopt bonding modes **C**, **E** and **G**.

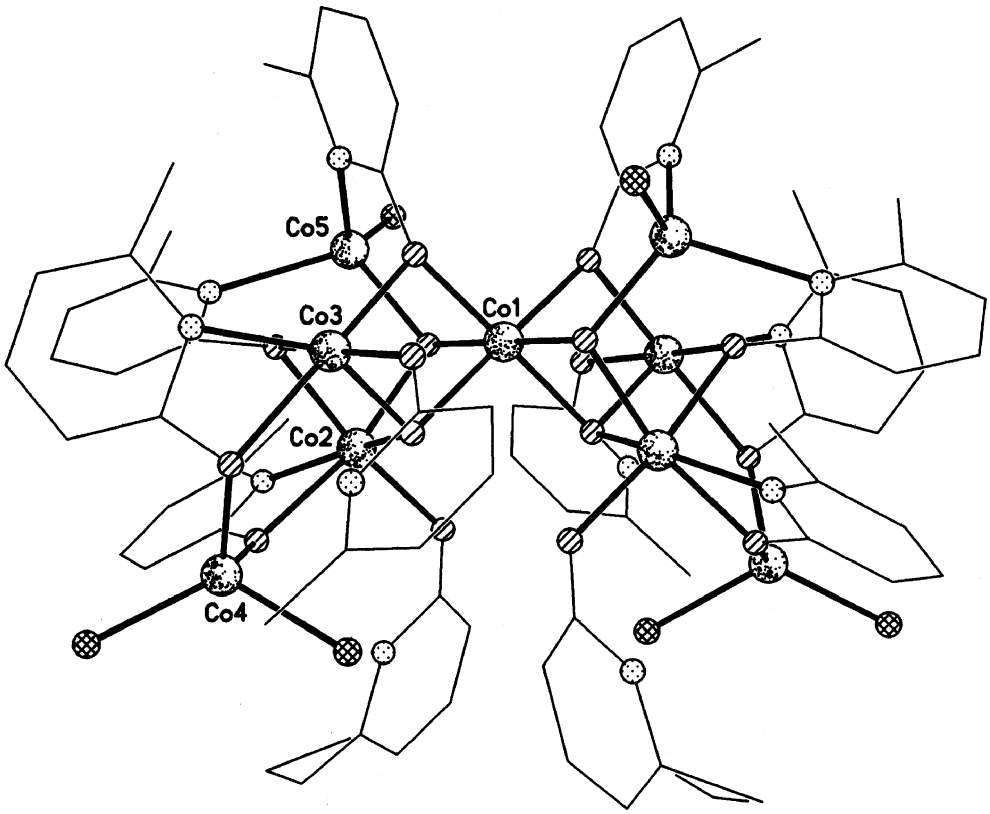

Figure 15. The structure of **13** in the crystal. A crystallographic two-fold axis passes through Co(1).

Attempting to make the nickel analogue of **12** failed entirely, generating a quite different cage $[Ni_4Na_4(mhp)_{12}(Hmhp)_2]$ **14** (figure 16) (Brechin *et al*. 1998*b*). This centrosymmetric structure features four chemically identical $[Ni(mhp)_3]^-$ units surrounding a central sodium 'chair'. Each mhp therefore chelates to the nickel site, and bridges on to either one or two sodium atoms. No hydroxide is found within the cage indicating that the nickel and cobalt chemistry is quite different in this system.

We have managed to incorporate hydroxide into a nickel-mhp cage, but by starting with nickel hydroxide and reacting that directly with 6-methyl-2-pyridone (Hmhp). The resulting cage is probably best written as $[Ni_6(OH)_6\{Ni(mhp)_3\}_5(Hmhp)(Cl)(H_2O)_2]$ **15** (figure 17) (Brechin *et al*. 1998*a*). As for **14**, $[Ni(mhp)_3]^-$ units are found attached to a central cage, but here the central cage is a $Ni_6(OH)_6$ face-sharing double-cubane (containing Ni(1), Ni(2), Ni(3), Ni(4), Ni(5) and Ni(6)). Two of the five $[Ni(mhp)_3]^-$ 'complex ligands' use all three O atoms to bind to nickel centres, while the remaining three units use two O atoms to bind nickel and the final oxygen to hydrogen-bond to hydroxide within the double-cubane core. This core resembles a small fragment of nickel oxide. The magnetic properties of **15** are disappointing; susceptibility studies indicate a low-spin ground state.

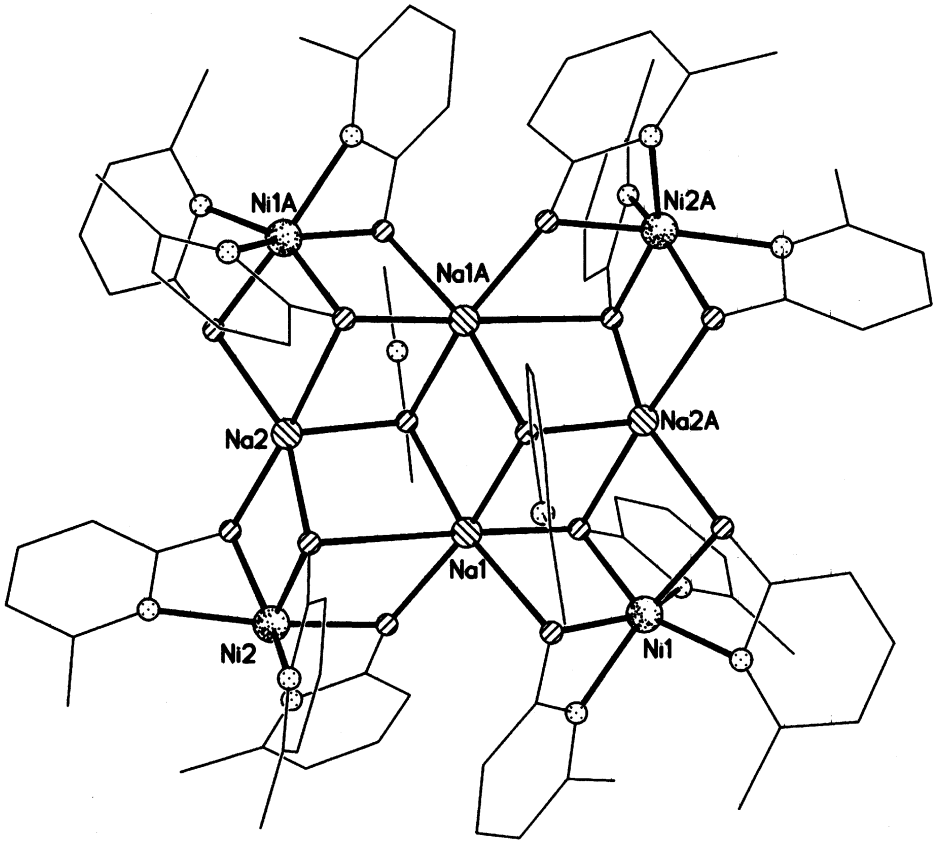

Figure 16. The structure of **14** in the crystal. The structure is centrosymmetric.

3. Discussion

Each of the three possible routes to high-nuclearity cages has advantages and disadvantages, which are worth considering.

Oligomerization induced by desolvation has the advantage that very compact cages result, with many short superexchange paths between metal centres. It appears to be applicable to a broad range of metal precursors and generates new structures. The main drawback with the approach is the lack of control of the structure of the resulting product. While some control seems possible by choice of temperature, this is likely to remain, in reality, rationalization of observations rather than a predictive tool.

Linking cages together through ligands such as phthalate is considerably more elegant, and offers more potential for control and prediction. Unfortunately, the disadvantage here is that the long superexchange path between cages can limit the magnetic communication as in **9**, and therefore although structurally a cage may be exciting, magnetically it may be rather dull. There are many obvious ways around this problem, including use of ligands which are stable radicals.

Serendipitous solvolysis produces the largest paramagnetic cages. It is related to the method by which very large polyoxometallates are produced, but is much less

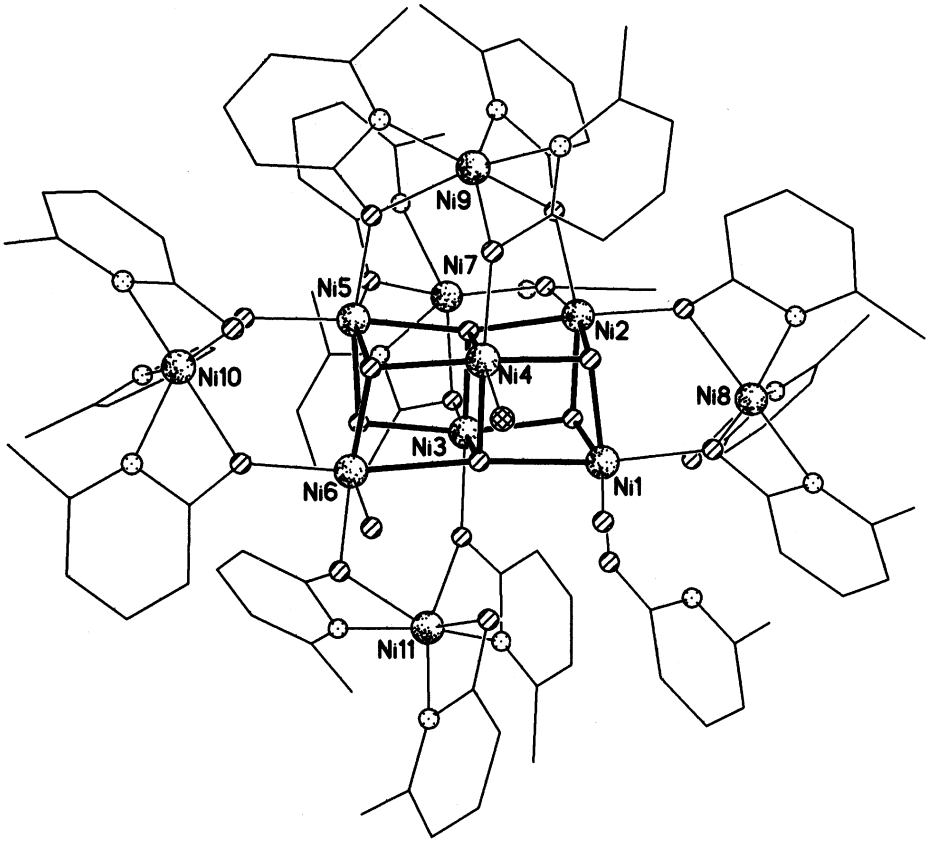

Figure 17. The structure of **15** in the crystal.

well developed at present. The main drawback here is reproducibility of conditions. Dependence on adventitious moisture can be extremely unreliable, but this problem should be comparatively straightforward to solve. There is a further drawback that the resulting structures are not controlled, although perhaps the resemblance of both **12** and **15** to minerals—cobalt hydroxide and nickel oxide, respectively—suggests that fragments of extended structures will be made through this route. On the positive side, in addition to the large cages which result, the superexchange pathways are short and lead to reasonably strong communications between spin centres.

This work was supported by the EPSRC(UK). Some of the crystallography was carried out by Sandy Blake, Robert Gould and Steven Harris (all Edinburgh). The EPR studies were performed by Eric McInnes and Frank Mabbs (Manchester), and Graham Smith (St. Andrews). Magnetic measurements were carried out in collaboration with Cristiano Benelli (Florence); this collaboration is supported by NATO.

References

Atkinson, I. M., Benelli, C., Murrie, M., Parsons, S. & Winpenny, R. E. P. 1999 Turning up the heat: synthesis of octanuclear chromium(III) carboxylates. *Chem. Commun.*, pp. 285–286.

Aubin, S. M. J., Wemple, M. W., Adams, D. M., Tsai, H.-L., Christou, G. & Hendrickson, D. N. 1996 Distorted $Mn^{IV}Mn_3^{III}$ cubane complexes as single-molecule magnets. *J. Am. Chem. Soc.* **118**, 7746–7754.

Aubin, S. M. J., Spagna, S., Eppley, H. J., Sager, R. E., Christou, G. & Hendrickson, D. N. 1998 Resonant magnetization tunnelling in the half-integer-spin single-molecule magnet $[PPh_4][Mn_{12}O_{12}(O_2CEt)_{16}(H_2O)_4]$. *Chem. Commun.*, pp. 803–804.

Barra, A. L., Debrunner, P., Gatteschi, D., Schulz, C. E. & Sessoli, R. 1996 Superparamagnetic-like behaviour in an octanuclear iron cluster. *Europhys. Lett.* **35**, 133–138.

Batsanov, A. S., Timko, G. A., Struchkov, Y. T., Gérbéléu, N. V. & Indrichan, K. M. 1991 Dodecanuclear chromium oxopivalate as the representative of new types of metal carboxylates: synthesis and structure. *Koord. Khim.* **17**, 662–669.

Blake, A. J., Brechin, E. K., Codron, A., Gould, R. O., Grant, C. M., Parsons, S., Rawson, J. M. & Winpenny, R. E. P. 1995 New polynuclear nickel complexes with a variety of pyridonate and carboxylate ligands. *J. Chem. Soc. Chem. Commun.*, pp. 1983–1985.

Blake, A. J., Gould, R. O., Grant, C. M., Milne, P. E. Y., Parsons, S. & Winpenny, R. E. P. 1997 Reactions of copper pyridonate complexes with hydrated lanthanoid nitrates. *J. Chem. Soc. Dalton Trans.* 485–495.

Brechin, E. K., Gould, R. O., Harris, S. G., Parsons, S. & Winpenny, R. E. P. 1996*a* Four cubes and an octahedron: a nickel–sodium supracage assembly. *J. Am. Chem. Soc.* **118**, 11 293–11 294.

Brechin, E. K., Harris, S. G., Parsons, S. & Winpenny, R. E. P. 1996*b* Desolvating cubes and linking prisms: routes to high nuclearity cobalt coordination assemblies. *Chem. Commun.*, pp. 1439–1440.

Brechin, E. K., Harris, S. G., Harrison, A., Parsons, S., Whittaker, A. G. & Winpenny, R. E. P. 1997 The synthesis and structural characterisation of a tetraicosanuclear cobalt complex. *Chem. Commun.*, pp. 653–654.

Brechin, E. K., Clegg, W., Murrie, M., Parsons, S., Teat, S. J. & Winpenny, R. E. P. 1998*a* Nanoscale cages of manganese and nickel with 'rock salt' cores. *J. Am. Chem. Soc.* **120**, 7365–7366.

Brechin, E. K., Gilby, L. M., Gould, R. O., Harris, S. G., Parsons, S. & Winpenny, R. E. P. 1998*b* Heterobimetallic nickel–sodium and cobalt–sodium complexes of pyridonate ligands. *Dalton Trans.* 2657–2664.

Fenske, D., Zhu, N. Y. & Langetege, T. 1998 Synthesis and structure of new Ag-Se clusters: $[Ag_{30}Se_8(Se^tBu)_{14}(P^n Pr_3)_8]$, $[Ag_{90}Se_{38}(Se^tBu)_{14}(PEt_3)_{22}]$, $[Ag_{114}Se_{34}(Se^nBu)_{46}(P^tBu_3)_{14}]$, $[Ag_{112}Se_{32}(Se^nBu)_{48}(P^tBu_3)_{12}]$ and $[Ag_{172}Se_{40}(Se^nBu)_{92}(dppp)_4]$. *Angew. Chem. Int. Ed. Engl.* **37**, 2640–2644.

Friedman, J. R., Sarachik, M. P., Tejada, J. & Ziolo, R. 1996 Macroscopic measurement of resonant magnetisation tunnelling in high-spin molecules. *Phys. Rev. Lett.* **76**, 3830–3833.

Halcrow, M. A., Sun, J. S., Huffman, J. C. & Christou, G. 1995 Structural and magnetic properties of $[Ni_4(\mu_3\text{-}OMe)_4(DBM)_4(MeOH)_4$ and $[Ni_4(\mu_3\text{-}N_3)_4(DBM)_4(EtOH)_4$: magnetostructural correlations for $[Ni_4X_4]^{4+}$ cubane complexes. *Inorg. Chem.* **34**, 4167–4177.

Müller, A., Krickemeyer, E., Bögge, H., Schmidtmann, M., Beugholt, C., Kögerler, P. & Lu, C. 1998 Formation of a ring-shaped reduced 'metal oxide' with the simple composition $[(MoO_3)_{176}(H_2O)_{80}H_{32}]$. *Angew. Chem. Int. Ed. Engl.* **37**, 1220–1223.

Sangregorio, C., Ohm, T., Paulsen, C., Sessoli, R. & Gatteschi, D. 1997 Quantum tunnelling of the magnetisation in an iron cluster nanomagnet. *Phys. Rev. Lett.* **78**, 4645–4648.

Sessoli, R., Gatteschi, D., Caneschi, A. & Novak, M. A. 1993*a* Magnetic bistability in a metal–ion cluster. *Nature* **365**, 141–143.

Sessoli, R., Tsai, H.-L., Schake, A. R., Wang, S., Vincent, J. B., Folting, K., Gatteschi, D., Christou, G. & Hendrickson, D. N. 1993*b* High-spin molecules: $[Mn_{12}O_{12}(O_2CR)_{16}(H_2O)_4]$. *J. Am. Chem. Soc.* **115**, 1804–1816.

Squire, R. C., Aubin, S. M. J., Folting, K., Streib, W. E., Hendrickson, D. N. & Christou, G. 1995 Octadecanuclearity in manganese carboxylate chemistry $K_4[Mn_{18}O_{16}(O_2CPh)_{22}(phth)_2(H_2O)_4]$ ($phthH_2$ = phthalic acid). *Angew. Chem. Int. Ed. Engl.* **34**, 887–889.

Sun, Z., Grant, C. M., Castro, S. L., Hendrickson, D. N. & Christou, G. 1998 Single-molecule magnets: out-of-phase AC susceptibility signals from tetranuclear vanadium(III) complexes with an $S = 3$ ground state. *Chem. Commun.*, pp. 721–722.

Thomas, L., Lionti, F., Ballou, R., Gatteschi, D., Sessoli, R. & Barbara, B. 1996 Macroscopic quantum tunnelling of magnetisation in a single crystal of nanomagnets. *Nature* **383**, 145–147.